John von Neumann Institute for Computing


# Application of Implicit Density Functionals to $3d$ Transition Metal Monoxides Dimension: Molecular Dynamics Simulations

R. N. Schmid, E. Engel, R. M. Dreizler

published in

*NIC Symposium 2001, Proceedings*,
Horst Rollnik, Dietrich Wolf (Editors),
John von Neumann Institute for Computing, Jülich,
NIC Series, Vol. **9**, ISBN 3-00-009055-X, pp. 213-223, 2002.



http://www.fz-juelich.de/nic-series/volume9

# Application of Implicit Density Functionals to $3d$ Transition Metal Monoxides

**R. N. Schmid, E. Engel, and R. M. Dreizler**

Institut für Theoretische Physik, J.W.Goethe-Universität Frankfurt
Robert-Mayer-Str.8-10, 60054 Frankfurt am Main, Germany
*E-mail: {rschmid, engel, dreizler}@th.physik.uni-frankfurt.de*

Standard density functional calculations on the basis of the local density approximation (LDA) predict the type II antiferromagnetic phases of FeO and CoO to be metallic, in contradiction to experiment. Within the framework of density functional theory this failure must be attributed to the shortcomings of the LDA, in particular to its incorrect treatment of the self-interaction. In this contribution we report results for FeO obtained with an implicit density functional including the exact exchange, which guarantees a complete elimination of the self-interaction.

## 1 Introduction

It is a long-standing question whether an effective single-particle description of Mott insulators is possible[1–4]. Although an enormous amount of work has been devoted to this question over the years (see e.g.[5–8]), a clear-cut answer is still not available. This is true not only for excitations and phase diagrams, but even for the ground states at $T = 0$. In this contribution we reconsider the ground state problem within density functional theory (DFT)[9], which currently is the most successful effective single-particle approach.

The prototype Mott insulators are the transition metal monoxides MnO, FeO, CoO and, in particular, NiO. In order to illustrate the challenge which these systems pose to a single-particle approach we consider NiO in more detail. Like MnO, FeO and CoO, NiO crystallizes in a rock salt structure with a lattice constant of 7.93 Bohr, as shown in Fig.1 (with a minor distortion in the case of FeO which will be ignored in the following). The basic features of the band structure of NiO, and thus its insulating property, can be understood as follows. The transition metal compounds typically exhibit a strong overlap

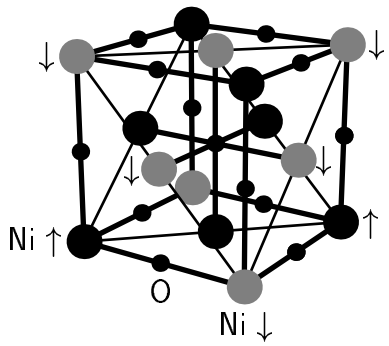


Figure 1. AFII structure of NiO.

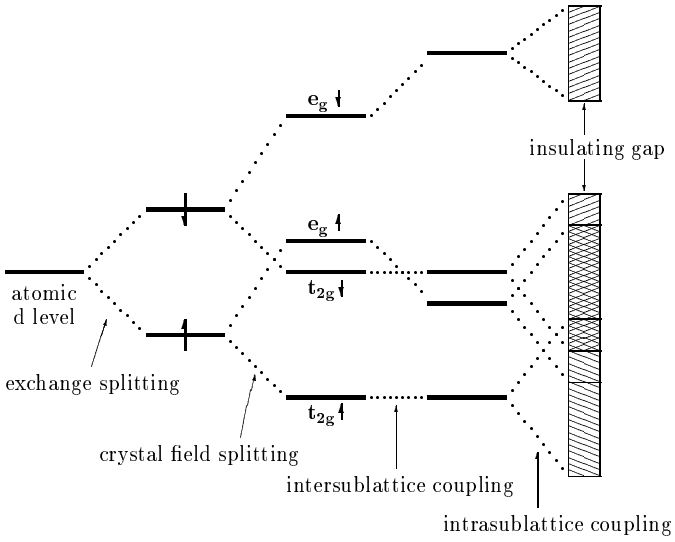


Figure 2. Band structure of Mott insulators: Qualitative picture of antiferromagnetic NiO.

of the metal $4s, 4p$ orbitals with their $r$-expectation values of about 3 Bohr and the oxygen $2s, 2p$ states. This leads to a strong hybridization of these states, so that the two $4s$ electrons of the metal are transferred to the oxygen $2p$ band and the gap between the $2s, 2p$ and the $4s, 4p$ bands becomes rather large. In between one finds, more or less well separated from the $2s, 2p$ and $4s, 4p$ bands, the $3d$ bands which, in the case of NiO, are occupied by 8 electrons per atom. The detailed structure of these bands can be explained by sequentially adding the various relevant effects to the $d$ level of an unpolarized atom[6], as illustrated in Fig.2. First of all, the exchange interaction splits the atomic level into a fully occupied, more strongly bound majority ($\uparrow$) and a partially occupied, less bound minority ($\downarrow$) spin level. For NiO this splitting is of the order of 1.6 eV. Next one has to take into account the octahedral symmetry of the lattice, i.e. the six doubly charged oxygen ions which surround each cation. This crystal field effect splits the five spatially distinct $d$ orbitals of each spin into an energetically lower triplet of $t_{2g}$ symmetry ($xy$, $yz$ and $zx$ character) and an energetically higher doublet of $e_g$ symmetry ($x^2 - y^2$ and $3z^2 - r^2$ character). The crystal field splitting is also of the order of 1 eV, so that no clear separation of up- and down-spin states emerges. At this point the description of NiO within a band theory framework seems to run into a fundamental problem: If one includes the periodicity of the system all subbands acquire a certain width $W$. Due to the small overlap of the $d$-orbitals from neighboring atoms the size of $W$ can be estimated on the basis of the tight binding method: One finds that $W$ is directly proportional to the nearest neighbor hopping integral and thus, indirectly, to the size of the crystal field splitting. As a result the $t_{2g}$ and $e_g$ subbands seem to overlap, so that a metallic state seems to emerge, in contradiction to experiment.

In order to understand the insulating nature of NiO its antiferromagnetic ordering has to be taken into account. All four transition metal monoxides of interest here are type II antiferromagnets (AFII) for which the majority spins of the atoms in (111) planes are

aligned, while the direction of the alignment alternates from plane to plane (see Fig.1), i.e. one has two magnetic sublattices and thus an effective doubling of the lattice constant. The impact of the antiferromagnetic structure on the $d$ bands can be extracted from an analysis of the relevant interaction hopping integrals, which characterize the coupling (and thus hybridization) of the $d$-states of neighboring Ni atoms. One finds that the strongest hopping integral is the $(dd\sigma)$-type coupling between second-nearest neighbor cations (along the cartesian axes) which is mediated by the $p_x$, $p_y$ and $p_z$ orbitals of the anions located in the middle between the cations[6]. As Fig.1 shows, the $(dd\sigma)$-interaction couples cations states of opposite polarization in the case of the AFII ordering. As a consequence the $(dd\sigma)$-interaction always links a majority spin $e_g$ state of one magnetic sublattice with a minority spin $e_g$ state in the other sublattice (intersublattice coupling). Their hybridization then leads to an energetic lowering of the occupied majority spin $e_g$ states of a given magnetic sublattice and a corresponding shift of the unoccupied minority spin $e_g$ states to higher energies. The $t_{2g}$-states, on the other hand, are not affected as they are fully occupied and only contribute to $(dd\pi)$- and $(dd\delta)$-coupling. The fact that the $(dd\sigma)$-interaction only couples cations from different sublattices is also responsible for the rather narrow width of the $e_g$ bands in the AFII structure (as compared with the width of the $t_{2g}$-bands or the ferromagnetic phase). Thus, combining the exchange and crystal field splittings with the antiferromagnetic hybridization shifts, the occupied bands are sufficiently well separated from the unoccupied $e_{g,\downarrow}$ band that the banding effect (intrasublattice coupling) cannot close the gap between these levels.

In the same fashion one can explain the insulating nature of MnO. In this case the large exchange splitting of roughly 3.8 eV is sufficient to produce a gap between the fully occupied majority spin $e_g$- and the completely unoccupied minority spin $t_{2g}$-band. None of the arguments above is in conflict with the single-particle picture, and, in fact, standard density functional calculations yield gaps for both NiO and MnO[6,7].

More difficult to describe with single-particle methods are the remaining two systems FeO and CoO for which the minority spin $t_{2g}$-band is partially occupied. Focusing on FeO, a single-particle description requires that for each site in a given sublattice two of the $t_{2g,\downarrow}$-states are empty, thus breaking the octahedral symmetry. For both spins the $t_{2g}$-level is thus split into a singly occupied state $t_{2g}^s$ (e.g. the $xy$-orbital) and a doubly degenerate level $t_{2g}^d$. The impact of this broken symmetry is most easily seen within the Hartree-Fock (HF) approximation[10]. In its most simple-minded version one can consider the $3d$ states in a net crystal field $v_{CF}$ produced by the nuclei and all other electrons. The single-particle energies $\epsilon_{k,\sigma}$ of the $d$-levels are then given by

$$\begin{aligned}\epsilon_{k,\sigma} = &\int d^3r\, \phi^\dagger_{k,\sigma}(\boldsymbol{r})\left\{\frac{-\boldsymbol{\nabla}^2}{2m} + v_{CF}(\boldsymbol{r})\right\}\phi_{k,\sigma}(\boldsymbol{r}) \\ &+e^2\sum_{l\tau}\Theta_{l\tau}[(k\sigma,l\tau||k\sigma,l\tau) - (k\sigma,l\tau||l\tau,k\sigma)]\,,\end{aligned} \tag{1}$$

where $\phi_{k,\sigma}$ represents the localized $d$-orbital of symmetry $k$ and spin $\sigma$, $\Theta_{k\sigma}$ denotes its occupation and $(ab||cd)$ is the standard Slater integral,

$$(k_1\sigma_1,k_2\sigma_2||k_3\sigma_3,k_4\sigma_4) = \int d^3r\, d^3r'\, \frac{\phi^\dagger_{k_1,\sigma_1}(\boldsymbol{r})\phi_{k_3,\sigma_3}(\boldsymbol{r})\phi^\dagger_{k_2,\sigma_2}(\boldsymbol{r}')\phi_{k_4,\sigma_4}(\boldsymbol{r}')}{|\boldsymbol{r}-\boldsymbol{r}'|}\,. \tag{2}$$

Starting from the atomic $d$-level, the first line of Eq.(1) leads to the $t_{2g}$ and $e_g$ states in the

crystal field. The differences between the two spin orientations and between occupied and unoccupied levels result from the second line. On a qualitative level the effect of the second line can be extracted within the most simple approximation to the relevant Slater integrals: Let $S$ denote the self-interaction energy of any of the 10 $d$ states, $U$ be the direct interaction between two spatially distinct states and $X$ be the corresponding exchange integral,

$$S = (k\sigma, k\tau||k\sigma, k\tau) \tag{3}$$
$$U = (k\sigma, l\tau||k\sigma, l\tau) \qquad (k \neq l) \tag{4}$$
$$X = (k\sigma, l\sigma||l\sigma, k\sigma) \qquad (k \neq l)\,. \tag{5}$$

This crudest possible approach ignores both the differences between the up- and down-orbitals and those between $t_{2g}$ and $e_g$ states. The second line of Eq.(1) then contributes to the eigenenergies of the various states as

$$t^d_{2g,\downarrow},\, e_{g,\downarrow} : (S + 5U) - X \tag{6}$$
$$t^s_{2g,\downarrow} : (2S + 4U) - S \tag{7}$$
$$t^s_{2g,\uparrow} : (2S + 4U) - (S + 4X) \tag{8}$$
$$t^d_{2g,\uparrow},\, e_{g,\uparrow} : (S + 5U) - (S + 4X)\,. \tag{9}$$

If one now takes into account the fact that $S, U >> X$ a gap of the order $U - X$ opens between the $t^s_{2g,\downarrow}$ level and the unoccupied states. Due to the strong localization of the $d$-states, which leads to a rather large $U$, this gap survives the broadening of the levels by the intrasublattice coupling. Thus, assuming that the coupling between the cells leads to a well-defined spatial pattern of occupied $t^s_{2g,\downarrow}$-states, this consideration shows that a single-particle description of FeO and CoO is not impossible.

An equivalent argument can be given in the case of DFT. In order to set the stage for the subsequent discussion let us first briefly summarize the essentials of DFT at this point.

## 2 Density Functional Theory

In DFT one uses the unique relation between the ground state of the system and its ground state density to recast the many-particle problem in the form of an auxiliary single-particle problem which reproduces the ground state density and energy of the actual many-body system exactly (but not its ground state)[9]. All complicated many-body effects are relegated to the so-called exchange-correlation (xc) energy $E_{xc}$ which, in the spin-dependent version of DFT (which we will use throughout this paper), is a universal (i.e. system-independent) functional of the spin-up ($n_\uparrow$) and spin-down ($n_\downarrow$) densities, $E_{xc}[n_\uparrow, n_\downarrow]$. The xc-energy is introduced as the difference between the exact ground state energy $E_{tot}$ of the interacting system and suitable single-particle components of $E_{tot}$,

$$E_{tot} = T_s[n_\uparrow, n_\downarrow] + \int d^3r\, v_n(\boldsymbol{r}) n(\boldsymbol{r}) + \sum_{\alpha<\beta} \frac{Z_\alpha Z_\beta e^2}{|\boldsymbol{R}_\alpha - \boldsymbol{R}_\beta|}$$
$$+ \frac{e^2}{2} \int d^3r \int d^3r'\, \frac{n(\boldsymbol{r}) n(\boldsymbol{r}')}{|\boldsymbol{r} - \boldsymbol{r}'|} + E_{xc}[n_\uparrow, n_\downarrow]\,. \tag{10}$$

Here $n = n_\uparrow + n_\downarrow$ is the total density, $v_n$ represents the potential of the nuclei at the positions $R_\alpha$,

$$v_n(\boldsymbol{r}) = -\sum_\alpha \frac{Z_\alpha e^2}{|\boldsymbol{r} - \boldsymbol{R}_\alpha|}\,, \tag{11}$$

and $T_s[n_\uparrow, n_\downarrow]$ is the kinetic energy of the auxiliary single-particle system. $T_s$ can be specified explicitly in terms of the single-particle orbitals $\phi_{k,\sigma}$ of the auxiliary problem which yields the exact spin-densities,

$$T_s = \frac{-1}{2m}\sum_{k,\sigma}\Theta_{k,\sigma}\int d^3r\,\phi^\dagger_{k,\sigma}(\boldsymbol{r})\boldsymbol{\nabla}^2\phi_{k,\sigma}(\boldsymbol{r}) \tag{12}$$

$$n_\sigma(\boldsymbol{r}) = \sum_k \Theta_{k,\sigma}|\phi_{k,\sigma}(\boldsymbol{r})|^2 \tag{13}$$

$$\Theta_{k,\sigma} = \begin{cases} 1 & \text{for } \epsilon_{k,\sigma} \le \epsilon_{F,\sigma} \\ 0 & \text{for } \epsilon_{F,\sigma} < \epsilon_{k,\sigma} \end{cases}\,. \tag{14}$$

The $\phi_{k,\sigma}$ are determined by a minimization of $E_{tot}$, Eq.(10), which leads to the single-particle equations of the auxiliary problem, the Kohn-Sham (KS) equations,

$$\left\{\frac{-\boldsymbol{\nabla}^2}{2m} + v_n(\boldsymbol{r}) + v_H([n];\boldsymbol{r}) + v_{xc,\sigma}([n_\uparrow, n_\downarrow];\boldsymbol{r})\right\}\phi_{k,\sigma}(\boldsymbol{r}) = \epsilon_{k,\sigma}\phi_{k,\sigma}(\boldsymbol{r})\,, \tag{15}$$

with the Hartree (H) and exchange-correlation (xc) potentials

$$v_H(\boldsymbol{r}) = e^2\int d^3r'\,\frac{n(\boldsymbol{r}')}{|\boldsymbol{r} - \boldsymbol{r}'|} \tag{16}$$

$$v_{xc,\sigma}(\boldsymbol{r}) = \frac{\delta E_{xc}[n_\uparrow, n_\downarrow]}{\delta n_\sigma(\boldsymbol{r})}\,. \tag{17}$$

Selfconsistent solution of Eqs.(13-17) with the exact $E_{xc}[n_\uparrow, n_\downarrow]$ leads to the exact $n_\sigma$ and $E_{tot}$ of the actually interesting system.

In view of the multiplicative nature of the potential in (15) the existence of a gap in FeO requires a strong spatial variation of $v_{xc,\downarrow}$: $v_{xc,\downarrow}$ must be much more attractive for the occupied $t^s_{2g,\downarrow}$-state than for the unoccupied $t^d_{2g,\downarrow}$-states. From Eqs.(6)-(9) it is clear that the driving force for the opening of a gap is the self-interaction correction component in the exchange energy: While it is present for the $t^s_{2g,\downarrow}$-state, it is missing for the $t^d_{2g,\downarrow}$-orbital. Thus the local manifestation of the self-interaction correction in $v_{xc,\downarrow}$ must be responsible for the spatial structure attracting the $t^s_{2g,\downarrow}$-state. It is thus no surprise that the most simple approximation for $E_{xc}[n_\uparrow, n_\downarrow]$, the local density approximation (LDA), predicts FeO and CoO to be metallic[7,8] (while the insulating ground states of MnO and NiO are correctly reproduced): The LDA, which treats the actual inhomogeneous system locally as if it was a homogeneous electron gas, is well known for its insufficient self-interaction correction in the atomic and molecular context[9].

Unfortunately, the standard extension of the LDA by inclusion of density gradients in the form of the generalized gradient approximation (GGA) does not really resolve the difficulties with FeO and CoO. Both the band structures and the magnetic moments obtained with the most frequently applied GGAs[11] are very similar to their LDA counterparts[7,8]. On the other hand, a GGA whose form has been optimized to reproduce atomic exchange

potentials as accurately as possible[12] does predict FeO and CoO to be antiferromagnetic insulators[8]. While the size of the gaps found is much too small, this result nevertheless provides a proof of principle that the mechanism described above can work in practice. Moreover, there is one further indication that the inappropriate handling of the self-interaction is responsible for the failure of the LDA: An explicitly self-interaction corrected form of the LDA gives the correct ground states[13].

This leads to the question whether an exact treatment of exchange is possible within DFT? The exact exchange energy functional $E_x$ is defined via the Fock expression, using the KS-orbitals[14,15],

$$E_x = -\frac{e^2}{2}\sum_\sigma \sum_{kl} \Theta_{k,\sigma}\Theta_{l,\sigma} \int d^3r \int d^3r' \, \frac{\phi^\dagger_{k,\sigma}(\boldsymbol{r})\phi_{l,\sigma}(\boldsymbol{r})\phi^\dagger_{l,\sigma}(\boldsymbol{r}')\phi_{k,\sigma}(\boldsymbol{r}')}{|\boldsymbol{r}-\boldsymbol{r}'|} \,. \quad (18)$$

Eq.(18) represents an implicit density functional as the $\phi_{k,\sigma}$ are unique functionals of $n_\sigma$ (this concept has already been used for $T_s$). Explicit use of (18) automatically guarantees the exact elimination of the self-interaction energy and should thus be ideally suited for the description of Mott insulators. The question which immediately arises in view of the orbital-dependent expression (18) is how to evaluate the corresponding xc-potential?

## 3 Optimized Potential Method

In contrast to the case of explicitly density-dependent functionals, for which the required functional derivative $\delta E_{xc}/\delta n_\sigma$ can be taken analytically, a more indirect, numerical procedure must be used for implicit functionals. The crucial equation of this so-called Optimized Potential Method (OPM)[16,17] is most easily derived by transforming the functional derivative with respect to $n_\sigma$ into a derivative with respect to $\phi_{k,\sigma}$, using the chain rule for functional differentiation. One ends up with a linear integral equation for $v_{xc,\sigma}$,

$$\int d^3r' \;\; \chi_{s,\sigma}(\boldsymbol{r},\boldsymbol{r}')v_{xc,\sigma}(\boldsymbol{r}') = \Lambda_{xc,\sigma}(\boldsymbol{r}) \,, \quad (19)$$

whose ingredients are the static response function of the KS auxiliary system,

$$\chi_{s,\sigma}(\boldsymbol{r},\boldsymbol{r}') = -\sum_k \Theta_{k,\sigma}\phi^\dagger_{k,\sigma}(\boldsymbol{r})G_{k,\sigma}(\boldsymbol{r},\boldsymbol{r}')\phi_{k,\sigma}(\boldsymbol{r}') + c.c. \quad (20)$$

$$G_{k,\sigma}(\boldsymbol{r},\boldsymbol{r}') = \sum_{l\neq k} \frac{\phi_{l,\sigma}(\boldsymbol{r})\;\phi^\dagger_{l,\sigma}(\boldsymbol{r}')}{\epsilon_{l,\sigma}-\epsilon_{k,\sigma}} \,, \quad (21)$$

and an inhomogeneity which contains the derivative $\delta E_{xc}/\delta\phi_{k,\sigma}$,

$$\Lambda_{xc,\sigma}(\boldsymbol{r}) = -\sum_k \int d^3r' \, \phi^\dagger_{k,\sigma}(\boldsymbol{r})G_{k,\sigma}(\boldsymbol{r},\boldsymbol{r}')\frac{\delta E_{xc}}{\delta\phi^\dagger_{k,\sigma}(\boldsymbol{r}')} + c.c. \,. \quad (22)$$

Eq.(19) determines $v_{xc,\sigma}$ only up to some additive constant, as

$$\int d^3r' \, \chi_{s,\sigma}(\boldsymbol{r},\boldsymbol{r}') = 0 \,. \quad (23)$$

The overall normalization of $v_{xc,\sigma}$ must be fixed by some additional constraint. Eq.(19) has to be solved selfconsistently together with the KS equations, i.e. its solution for fixed $\phi_{k,\sigma}$

| Atom | $E_{tot}$ | $E_{tot} - E_{tot}^{OPM}$ | | | |
|---|---|---|---|---|---|
| | OPM | KLI | LDA | GGA | HF |
| He | −2861.7 | 0.0 | 138.0 | 6.5 | 0.0 |
| Be | −14572.4 | 0.1 | 349.1 | 18.2 | −0.6 |
| Ne | −128545.4 | 0.6 | 1054.7 | −23.5 | −1.7 |
| Mg | −199611.6 | 0.9 | 1362.8 | −0.5 | −3.1 |
| Ar | −526812.2 | 1.7 | 2294.8 | 41.2 | −5.3 |
| Ca | −676751.9 | 2.2 | 2591.8 | 25.7 | −6.3 |
| Zn | −1777834.4 | 3.7 | 3924.5 | −252.6 | −13.8 |
| Kr | −2752042.9 | 3.2 | 5176.8 | −18.4 | −12.0 |

Table 1. Exchange-only ground state energies of neutral atoms with closed sub-shells: OPM results[23] versus KLI, LDA, PW91-GGA[11] and HF[24] results (all energies in mHartree).

replaces the insertion of $n_\sigma$ into conventional xc-functionals. Eqs.(19)-(23) have been formulated for arbitrary implicit xc-functionals, including a possible correlation component $E_c$. However, to date no suitable orbital-dependent approximation for $E_c$ is available, so that the exact $E_x$ is usually combined with a standard density functional for $E_c$[18–21].

The evaluation of $\chi_{s,\sigma}$ is computationally rather demanding, as a large number of excited states have to be taken into account in the evaluation of the Greens function (21). Thus an approximate (semi-analytical) solution of Eq.(19) is obviously of interest. Such a solution can be obtained by use of a closure approximation for $G_{k,\sigma}$, which leads to the Krieger-Li-Iafrate approximation (KLI)[16,22] to the OPM,

$$v_{xc,\sigma}^{KLI}(\boldsymbol{r}) = \frac{1}{2n_\sigma(\boldsymbol{r})} \sum_k \left\{ \left[ \phi_{k,\sigma}^\dagger(\boldsymbol{r}) \frac{\delta E_{xc}}{\delta \phi_{k,\sigma}^\dagger(\boldsymbol{r})} + c.c. \right] + |\phi_{k,\sigma}(\boldsymbol{r})|^2 \Delta v_{k,\sigma} \right\} \quad (24)$$

$$\Delta v_{k,\sigma} = \int d^3r \left\{ \Theta_{k,\sigma} |\phi_{k,\sigma}(\boldsymbol{r})|^2 v_{xc,\sigma}^{KLI}(\boldsymbol{r}) - \phi_k^\dagger(\boldsymbol{r}) \frac{\delta E_{xc}}{\delta \phi_{k,\sigma}^\dagger(\boldsymbol{r})} \right\} + c.c. \; . \quad (25)$$

Eqs.(24),(25) can either be solved iteratively or resolved via a set of linear equations for the unknown component of the right-hand side, $\int d^3r |\phi_k|^2 v_{xc}$.

The accuracy of the KLI approximation is most easily demonstrated for atoms. In Table 1 we list the ground state energies obtained with the exact $E_x$, either on the basis of the full OPM or with the KLI-approximation, as well as with the LDA and a widely used GGA[11] for a number of atoms. In all calculations correlation has been neglected (x-only limit). For comparison the corresponding HF numbers are also given. Table 1 demonstrates that x-only OPM and HF energies are very close to each other, reflecting the limited importance of the nonlocality of the HF exchange potential for the variational freedom (in both cases the same energy expression is minimized). More important in the present context is the observation that the KLI-approximation is extremely accurate. The LDA and GGA, on the other hand, exhibit the well-known deviations from the exact result.

The accuracy of the KLI-approximation can also be examined on a more microscopic level by analyzing the exchange potential itself. In Fig.3 we plot the exchange potentials obtained by selfconsistent OPM, KLI, LDA and GGA calculations for neon. For all $r$ the KLI potential is very close to the exact OPM result. Only the very pronounced shell-structure in the OPM potential is smoothed out (note, however, that this feature is

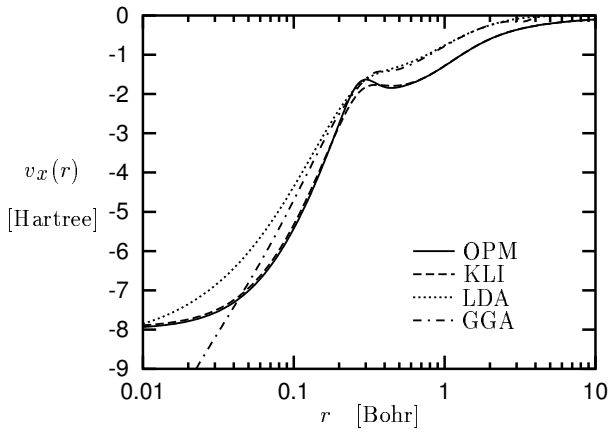


Figure 3. Exchange potential of Atoms: KLI approximation versus full OPM solution. Selfconsistent OPM, KLI, LDA and GGA results for Ne.

completely absent in the LDA and GGA potential). The OPM and KLI potentials are particularly close in the asymptotic regime, in which they both decay like $-1/r$. This behavior reflects the fact that both potentials are self-interaction free (compare[25]). An analogous comparison for metallic aluminum is provided by Fig.4. Again the accuracy of the KLI-approximation is apparent. One can thus reliably replace the solution of Eq.(19) by the KLI form (24).

## 4 Application of Exact $E_x$ to FeO

In order to study the implications of the exact exchange for the transition metal oxides we have applied the combination of the exact $E_x$ with the LDA for correlation to the AFII structure of FeO. In view of the enormous computational demands of an OPM calculation for this system we have resorted to (a) the KLI approximation and (b) a pseudopotential approach (analogous to[19,21]). The valence space consisted of the iron $3p$, $3d$ and $4s$ states. Normconserving pseudopotentials of Troullier-Martins type[26] have been used (compare[27]). A plane-wave basis with an energy cut-off of 250 Ryd was required for an accurate description of the $3p$ states. Test calculations with the LDA showed that 3 special $k$-points were sufficient for the integration over the Brillouin zone[28].

The resulting band structure is shown in Fig.5. As in the case of the LDA, a metallic ground state is found. On the other hand, many details of the band structure are rather different from the LDA result (compare[7,8]). In particular, the exact $E_x$ reproduces the separation of the oxygen $2p$ from the iron $3d$ bands observed in experiment[29]. The same effect has been seen in a calculation with the exact $E_x$ for MnO[20].

In view of this somewhat ambiguous result the question arises to what extent the technical limitations of the calculation might affect the band structure. As we have demonstrated the accuracy of the KLI-approximation in Section 3 and explicitly verified by LDA calculations that the basis set size and the Brillouin zone sampling are sufficient, only two aspects appear to be worth a closer examination. On the one hand, there are indications

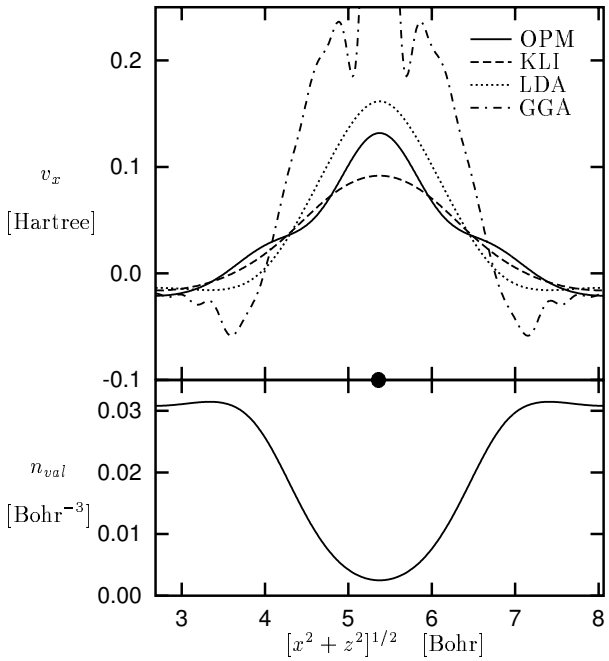


Figure 4. Exchange potential of Al along [110]-direction from plane-wave pseudopotential calculation: Exact OPM exchange potential versus KLI approximation, LDA and PW91-GGA (in all cases the selfconsistent density obtained with the KLI approximation has been used for the evaluation of $v_x[n]$). Also shown is the corresponding valence density (44 special $k$-points, $E_{cut} = 100Ryd$ for basis, $E_{cut} = 50Ryd$ for OPM equation).

that the combination of the exact $E_x$ with the LDA for $E_c$ suffers from the overestimation of correlation energies and potentials by the LDA (in a pure LDA calculation this effect fortuitously cancels with the LDA's underestimation of exchange energies and potentials[25]). However, as the discussion of Section 1 identifies the exchange as the component which is responsible for the opening of the gap, it is unlikely that the failure of the present calculation is due to the shortcomings of the LDA for $E_c$.

On the other hand, the exclusion of the $3s$ electrons from the valence space seems to be critical: It is well known from LDA pseudopotential calculations for iron that the $3s$ electrons must be included (at least in the form of nonlinear core corrections — compare[30,31]). This fact is illustrated in Fig.6 where the spin-up eigenvalues of diatomic FeO are shown. The all-electron values are compared with three pseudopotential results, based on different valence spaces (the LDA is utilized for this comparison as all-electron OPM results for FeO are not available). It is obvious that the levels obtained with the $3p3d4s$-type valence space are much less realistic than those found with the more complete valence space including the $3s$ electrons (nonlinear core corrections are not used). A detailed study of the ground and lowest excited states of FeO shows that the excitation energies of this molecule depend very sensitively on the size of the valence space[31]. In fact, with the $3p3d4s$-type valence space an incorrect ground state is predicted if nonlinear core corrections are not included (as in our OPM calculation for solid FeO). On the other hand, the $3s3p3d4s$ valence space

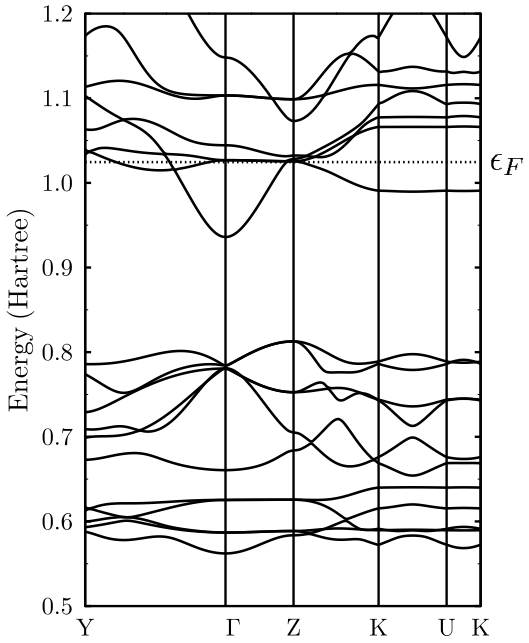


Figure 5. Band structure of FeO in AFII structure ($a = 8.145$ Bohr): Plane-wave-pseudopotential calculation with exact $E_x$, using (a) the KLI-approximation, (b) the LDA for $E_c$, (c) $E_{cut} = 250$ Ryd, (d) a valence space including the iron $3p$, $3d$ and $4s$ states, (e) no nonlinear core corrections.

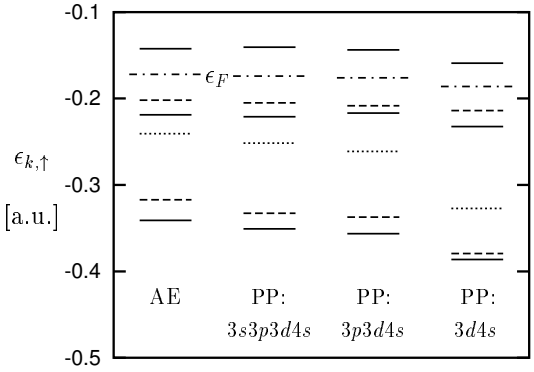


Figure 6. Spin-up eigenvalues of diatomic FeO (for $R = 3.0$ Bohr): Various pseudopotentials (PP) without nonlinear core corrections in comparison with all-electron (AE) result ($\sigma$-levels — solid lines, $\pi$-levels — dashed lines, $\delta$-levels — dotted lines).

yields the correct ground state. A definitive conclusion concerning the importance of the exact $E_x$ for the insulating nature of FeO thus requires the inclusion of the $3s$ states, in spite of the resulting increased computational demands.

## Acknowledgments

Computer time for this work has been provided by the John-von-Neumann Institute for Computing at the Research Centre Jülich and the Hochschulrechenzentrum of the Univ. of Frankfurt. Financial support by the Deutsche Forschungsgemeinschaft (grant Dr 113/20-3) is gratefully acknowledged.

## References

1. N. F. Mott, Proc. Roy. Soc. (London) **A62**, 416 (1949).
2. J. C. Slater, Phys. Rev. **82**, 538 (1953).
3. P. W. Anderson, Phys. Rev. **115**, 2 (1959).
4. J. Hubbard, Proc. Roy. Soc. (London) **A276**, 238 (1963).
5. T. M. Wilson, Int. J. Quantum Chem. Symp. **3**, 757 (1970).
6. K. Terakura, T. Oguchi, A. R. Williams, and J. Kübler, Phys. Rev. B **30**, 4734 (1984).
7. T. C. Leung, C. T. Chan, and B. N. Harmon, Phys. Rev. B **44**, 2923 (1991).
8. P. Dufek, P. Blaha and K. Schwarz, Phys. Rev. B **50**, 7279 (1994).
9. R. M. Dreizler and E. K. U. Gross, *Density Functional Theory*, (Springer, Berlin, 1990).
10. B. H. Brandow, Adv. Phys. **26**, 651 (1977).
11. J. P. Perdew, J. A. Chevary, S. H. Vosko, K. A. Jackson, M. R. Pederson, D. J. Singh, and C. Fiolhais, Phys. Rev. B **46**, 6671 (1992).
12. E. Engel and S. H. Vosko, Phys. Rev. B **47**, 13164 (1993).
13. A. Svane and O. Gunnarsson, Phys. Rev. Lett. **65**, 1148 (1990).
14. V. Sahni, J. Gruenebaum, and J. P. Perdew, Phys. Rev. B **26**, 4371 (1982).
15. D. C. Langreth and M. J. Mehl, Phys. Rev. B **28**, 1809 (1983).
16. R. T. Sharp and G. K. Horton, Phys. Rev. **90**, 317 (1953).
17. J. D. Talman and W. F. Shadwick, Phys. Rev. A **14**, 36 (1976).
18. T. Kotani, Phys. Rev. Lett. **74**, 2989 (1995).
19. D. M. Bylander and L. Kleinman, Phys. Rev. Lett. **74**, 3660 (1995).
20. T. Kotani and H. Akai, Phys. Rev. B **54**, 16502 (1996).
21. M. Städele, J. A. Majewski, P. Vogl, and A. Görling, Phys. Rev. Lett. **79**, 2089 (1997).
22. J. B. Krieger, Y. Li and G. J. Iafrate, Phys. Lett. **146** A, 256 (1990).
23. E. Engel and S. H. Vosko, Phys. Rev. A **47**, 2800 (1993).
24. C. Froese Fischer, *The Hartree-Fock Method for Atoms* (Wiley, New York, 1977).
25. E. Engel and R. M. Dreizler, J. Comput. Chem. **20**, 31 (1999).
26. N. Troullier and J. L. Martins, Phys. Rev. B **43**, 1993 (1991).
27. E. Engel, A. Höck, R. N. Schmid, R. M. Dreizler and N. Chetty, Phys. Rev. B **64**, 125111 (2001).
28. H. J. Monkhorst and J. D. Pack, Phys. Rev. B **13**, 5188 (1976).
29. D. E. Eastman and J. L. Freeouf, Phys. Rev. Lett. **34**, 395 (1975).
30. P. Ballone and R. O. Jones, Chem. Phys. Lett. **233**, 632 (1995).
31. E. Engel, A. Höck, and R. M. Dreizler, Phys. Rev. B **63**, 125121 (2001).